Journal of Hazardous Materials 261 (2013) 621–627

Contents lists available at ScienceDirect

Journal of Hazardous Materials

journal homepage: www.elsevier.com/locate/jhazmat

Arsenite removal from aqueous solution by a microbial fuel cell–zerovalent iron hybrid process

An Xue[a,b], Zhong-Zheng Shen[a,b], Bin Zhao[c,d], Hua-Zhang Zhao[a,b,*]

[a] Department of Environmental Engineering, Peking University, Beijing 100871, China
[b] The Key Laboratory of Water and Sediment Sciences, Ministry of Education, Beijing 100871, China
[c] School of Environmental and Chemical Engineering, Tianjin Polytechnic University, Tianjin 300160, China
[d] State Key Laboratory of Hollow Fiber Membrane Materials and Processes, Tianjin 300160, China

ARTICLE INFO

Article history:
Received 11 March 2013
Received in revised form 20 July 2013
Accepted 22 July 2013
Available online 7 August 2013

Keywords:
Arsenite
Zerovalent iron
Microbial fuel cell
Arsenic removal
Electrosorption

ABSTRACT

Conventional zerovalent iron (ZVI) technology has low arsenic removal efficiency because of the slow ZVI corrosion rate. In this study, microbial fuel cell (MFC)–zerovalent iron (MFC–ZVI) hybrid process has been constructed and used to remove arsenite (As(III)) from aqueous solutions. Our results indicate that the ZVI corrosion directly utilizes the low-voltage electricity generated by MFC in the hybrid process and both the ZVI corrosion rate and arsenic removal efficiency are therefore substantially increased. The resultant water qualities are compliant with the recommended standards of EPA and WHO. Compared to the ZVI process alone, the H_2O_2 generation rate and output are dramatically improved in MFC–ZVI hybrid process. Strong oxidants derived from H_2O_2 can rapidly oxidize As(III) into arsenate (As(V)), which helps to improve the As(III) removal efficiency. The distribution analysis of As and Fe indicates that the As/Fe molar ratio of the flocs in solution is much higher in the MFC–ZVI hybrid process. This phenomenon results from the different arsenic species and hydrous ferric oxides species in these two processes. In addition, the electrosorption effect in the MFC–ZVI hybrid process also contributed to the arsenic removal by concentrating As(V) in the vicinity of the iron electrode.

1. Introduction

Arsenic contamination of water has been a worldwide concern due to the toxicity and carcinogenicity of various arsenic species [1–3]. The predominant species in natural water are inorganic arsenate (As(V)) and arsenite (As(III)). As(III) exists not only in groundwater, but also widely in surface water and sediment [4–7]. Compared to As(V), As(III) is more mobile and 25–60 times higher in toxicity. The concentrated As(III) in sediment is released continuously into surface water due to the presence of a reducing environment, which renders the task of As(III) removal protracted and arduous [4,8]. Conventional techniques for arsenic removal, e.g., coagulation, precipitation and adsorption, are generally less effective for As(III) than for As(V) [3,9,10]. Therefore, studies on As(III) removal are becoming a focus in arsenic pollution research especially in drinking water treatment.

For efficient arsenic removal, oxidation of As(III) to As(V) has been suggested [9,11,12]. Arsenic removal by zerovalent iron (ZVI) technology, a facile and economical process, can simultaneously oxidize and remove As(III) [11,13–15]. The ZVI corrosion process in water releases Fe^{2+} ions, which undergo a series of oxydrolysis and finally generate many types of hydrous ferric oxides (HFOs). During this process, arsenic can be removed by means of adsorption and coprecipitation [16]. The newly formed HFOs are generally considered more effective for the pollutant removal as compared to the iron coagulants added directly [10,17]. Moreover, when the Fe^{2+} released from the ZVI process is further oxidized to Fe^{3+} by O_2, oxidants (H_2O_2, $^{\bullet}OH$) are also generated at the same time. These oxidants can oxidize As(III) to As(V), and the latter is usually more easily removed by adsorption [3,14]. The ZVI corrosion rate directly determines the generation rates of both HFOs and oxidants, and therefore affects the arsenic removal efficiency in the ZVI process. According to the electrolytic theory, the ZVI will not corrode unless an electric current goes through the electrolyte in the system. The corrosion rate depends on the potential difference between the cathode and the anode as well as the conductivity of the electrolyte solution [18]. Since the potential differences between different sites on the ZVI surface are small, the ZVI corrosion rate is therefore quite slow. As a consequence, the arsenic removal efficiency is seriously restricted.

A microbial fuel cell (MFC) is a device that uses bacteria as the catalysts to oxidize organic and inorganic matter in the environment to produce electricity [19–22]. Sediment microbial fuel cell

* Corresponding author at: Department of Environmental Engineering, Peking University, Beijing 100871, China. Tel.: +86 10 62754292x815; fax: +86 10 62756526.
E-mail address: zhaohuazhang@pku.edu.cn (H.-Z. Zhao).

0304-3894/$ – see front matter © 2013 Elsevier B.V. All rights reserved.
http://dx.doi.org/10.1016/j.jhazmat.2013.07.072

(SMFC) and benthic microbial fuel cell (BMFC) are the types that generate modest levels of electrical power in sediment or seafloor environments by a mechanism analogous to the coupled biogeochemical reactions that transfer electrons from organic carbon through redox intermediates to oxygen [23,24]. Due to the limitation of the theoretical electrogenesis voltage of the MFC (on the order of 1.1 V) and the possible losses, the maximum open circuit voltage of MFC is typically less than 0.8 V [19,25]. Even in the latest microbial reverse-electrodialysis cell (MRC), the maximum voltage generated is around 1.2–1.3 V [26]. Stacking MFCs in series can improve the voltage output [27,28]. However, the advantage gained by increasing the number of series-stacked MFCs may be offset by the concomitant electric energy loss [29]. The inferior capability of power generation in the MFCs seriously restricts their applications. Currently, MFCs are mainly used to power miniwatt devices under particular circumstances. One example exploited the voltage difference between the cathode in oxygen rich water and the anode in anaerobic substrate sludge by means of BMFC to power sensors in the ocean [30].

When the MFC is coupled with other instruments or technologies, direct utilization of the generated electricity without electricity collection is possible because of the specific structure of the MFC and its electricity generation characteristics [31]. For example, the MFC can be used to treat the wastewater containing NO_3^-, CrO_4^{2-}, Cu^{2+}, etc. [32–34]. Modified MFC can also be used in seawater desalination, in which the potential difference generated in the MFC was directly used to separate the anions from cations in seawater [35,36]. These novel ways of MFC utilization not only make full use of the electrons and electricity generated in the MFC, but also expand its range of application.

The marriage of the MFC and ZVI technologies would potentially provide an efficient way of utilizing the low electricity generated by the MFCs for driving the ZVI corrosion process. To the best of our knowledge, no study on the MFC–ZVI hybrid process has been reported.

In this paper, we provide proof of concept of the MFC–ZVI hybrid system for As(III) removal from aqueous solutions. The unique characteristics of this hybrid system as compared to the ZVI process are discussed. The underlying mechanism in the As(III) removal process is investigated in terms of the As(III) removal efficiency, the production of HFOs and H_2O_2 and the distribution profiles of the arsenic and iron in the process.

2. Materials and methods

2.1. Construction and operation of the MFC

A single-chamber MFC, 125 cm^3 in volume of slab geometry, 5 cm × 5 cm × 5 cm, was used in this work. Carbon paper containing a Pt catalyst (0.5 mg cm^{-2}) on the water-facing side (4 cm × 4 cm (16 cm^2), Feichilvneng Co., Beijing, China), as the air cathode, was connected to the external circuit by a copper mesh (100 mesh, Hiway Co., Beijing, China). Non-wet-proofed carbon felt (4 cm × 4 cm (16 cm^2), 3 mm thick, Beijing Evergrow Resources Co., Ltd., China) was used as the anodes. The MFC was inoculated with anaerobic sludge (collected from Xiaojiahe Wastewater Treatment Plant in Beijing, China, 50% v/v) and fed with a synthetic medium. The medium composition was as follows (per liter): glucose, 800 mg; $NaH_2PO_4{\cdot}2H_2O$, 5620 mg; $Na_2HPO_4{\cdot}12H_2O$, 6150 mg; NH_4Cl, 310 mg; KCl, 130 mg; a mineral solution of 12.5 mL [37]. The MFC was operated at a room temperature of 25 ± 3 °C. The performance of the working MFC was characterized by polarization curves and power density curves. Polarization curves were obtained using an adjustable external resistance. Power and current were calculated based on the following equations:

$$P = I \times E \quad (1)$$

$$I = \frac{E}{R_{ext}} \quad (2)$$

where P is the generated power; E is the measured cell voltage; R_{ext} is the external resistance, and I is the produced current. The online recorded produced current and power were normalized by the surface area of the used anode. Columbic efficiency (CE) can be calculated as follows [38].

$$CE = \frac{C_P}{C_T} \times 100 \quad (3)$$

where C_P is obtained by integrating the current variation over time and C_T is the theoretical amount of coulombs that can be produced from the carbon source (i.e., glucose).

2.2. Arsenite removal experiment

The chemicals were of analytical reagent grade and used without further purification. The test solution containing 300 μg/L arsenic was prepared by adding a proper amount of As_2O_3 into the tapwater obtained from Peking University. The pH value of the test solution is 8.0. Its compositions are shown in Table S1 in Supporting information. Other solutions were prepared using Milli-Q (18.2 MΩ cm) water.

Arsenite removal was conducted using the MFC–ZVI hybrid process and the ZVI process, respectively. The ZVI process was composed of a beaker (250 mL) and two electrodes. Anode was made of high purity iron (2.5 cm × 2.5 cm (6.25 cm^2), 5 mm thick, Mengtai Co., Beijing, China) and cathode was made of carbon felt (2.5 × 2.5 cm (6.25 cm^2), 3 mm thick, Beijing Evergrow Resources Co., Ltd., China). The distance between the two electrodes immersed in water was 0.7 cm. Before the experiment, high purity iron electrode was polished by a sand paper and rinsed in 1 N H_2SO_4 followed by deionized water. This process should be repeated if the electrode is used again. During the experiments, air was pumped (2 W, Hibive Co., Hangzhou, China) into the cathode region at a flux of about 500 mL/min. The distance between the two electrodes, specific surface area of anode, cathode material and other parameters of the ZVI process may affect the arsenic removal efficiency. For the objective of the study is to provide a proof of the concept of the MFC–ZVI hybrid system for As(III) removal from aqueous solutions, these parameters were kept constant in this study. The MFC–ZVI hybrid process was set up by coupling the MFC with the ZVI process and its schematic is shown in (Fig. 1). The cathode of the MFC was connected to the high purity iron anode of the ZVI process, while the anode of the MFC was connected to the carbon felt cathode of the ZVI process. The current going through the MFC–ZVI hybrid process was obtained by measuring the voltage over a 10 Ω resistance connected into the circuit (Eq. (2)).

200 mL test solution was used in each test. The air pump was started as soon as the entire circuit was completed. Samples were taken by syringes at regular intervals for the analysis of As(III) and total arsenic (As(tot)). Each test was repeated three times, and the average was used for data analysis.

2.3. H_2O_2 and Fe(tot) determination

Fe(II) generated by ZVI corrosion can react with H_2O_2, which results in the consumption of H_2O_2 and the production of HFOs. In order to get the accurate amount of H_2O_2 and total Fe (Fe(tot)) generated in both processes, a specific experiment was conducted by adding 5 μM 2,2′-bipyridyl (BPY) into the reaction system to

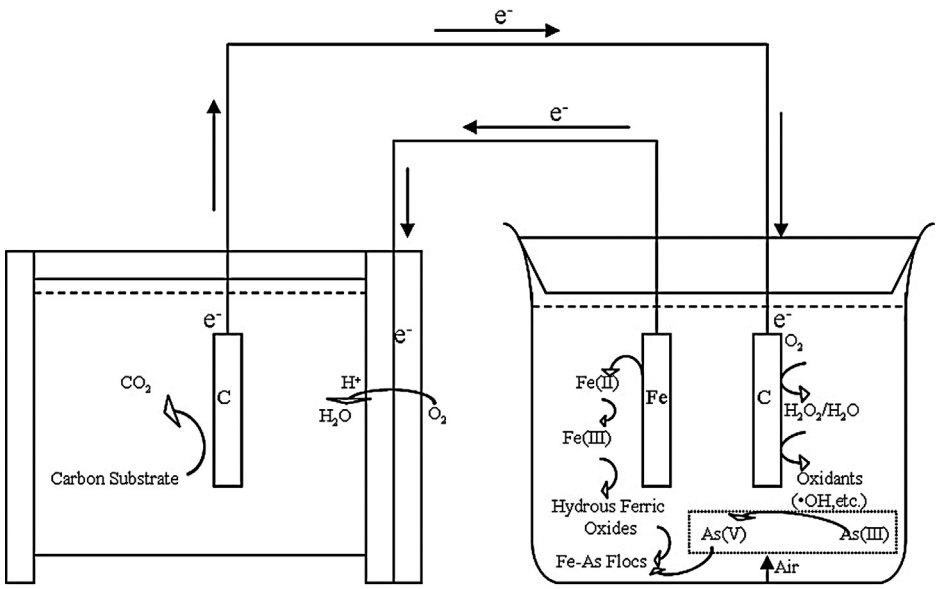

Fig. 1. Schematic of the MFC–ZVI hybrid process.

prevent the action between Fe(II) and H_2O_2 [14,39]. Samples were taken by syringes at regular intervals to determine the concentrations of H_2O_2 and Fe(tot).

2.4. Speciation distribution of As and Fe

Speciation of As and Fe in both the MFC–ZVI hybrid process and the ZVI process was quantitatively investigated according to the method published in our previous studies [40,41]. Arsenic in both MFC–ZVI and ZVI processes was divided into three parts: the part remaining in the solution ($[As]_{solution}$), the part retained on the electrodes ($[As]_{electrodes}$), and the part removed by flocs ($[As]_{flocs}$). The initial arsenic concentration was denoted as $[As]_{initial}$. One part of the sample used for the As and Fe distribution analysis was filtered through a 0.45-μm membrane. The arsenic concentration in the filtration was denoted as $[As]_{solution}$. The other part of the sample for the As and Fe distribution analysis was acidified with a HNO_3 solution to pH < 1 in order to completely dissolve the flocs and release the As into the solution. The arsenic concentration in the acidified solution was denoted as ($[As]_{solution+flocs}$). According to the above definitions, $[As]_{flocs}$ and $[As]_{electrodes}$ can be obtained by Eqs. (4) and (5):

$$[As]_{flocs} = [As]_{solution+flocs} - [As]_{solution} \quad (4)$$

$$[As]_{electrodes} = [As]_{initial} - [As]_{solution+flocs} \quad (5)$$

Similarly, the Fe in the system was also divided into $[Fe]_{solution}$, $[Fe]_{electrodes}$, and $[Fe]_{flocs}$. The pretreatment methods of samples were the same as in the As distribution analysis.

2.5. Analysis

Modified N,N-diethyl-p-phenylenediamine (DPD) method was used to determine the concentration of H_2O_2 [14]. The concentration of Fe including Fe(tot) was measured by an ICP-AES (OPTIMA2000, PerkinElmer). As(III) analysis was performed using Liquid Chromatography–Atom Fluorescence Spectrometer (LC-10AT VP Plus, Shimadzu; AFS-9130, Jitian Instrument Co., Ltd., China). Total arsenic concentrations were determined by an ICP-MS (X Series II, Thermo). The pH was measured by a pH meter (pH-201, Hanna).

3. Results and discussion

3.1. MFC performance

The power generation property of the single-chamber MFC used in this work is shown in Fig. 2. The inner resistance of the MFC is calculated to be 108 Ω. The maximum power density output at 477 mW/m^2 is obtained when the electricity density is at 1726 mA/m^2. With a 1000 Ω resistor into the outer circuit, the maximum steady voltage output is measured to be 0.52 V and the Columbic efficiency 4.59% during the power generation process. The performance of the MFC in the present study is comparable to other similar MFCs in the literatures [42,43].

3.2. Arsenite removal

Fig. 3 shows the arsenic removal kinetics in the MFC–ZVI hybrid process and the ZVI process. Both the As(III) and As(tot) concentrations decrease much faster in the MFC–ZVI hybrid process than in the ZVI process. For the MFC–ZVI hybrid process, the As(tot) concentration remaining in solution is only 9.8 μg/L and the As(III) concentration is below detection limit after 2 h. The treated water qualities are compliant with the recommended standards of EPA and WHO (10 μg/L). However, for the ZVI process, there are a

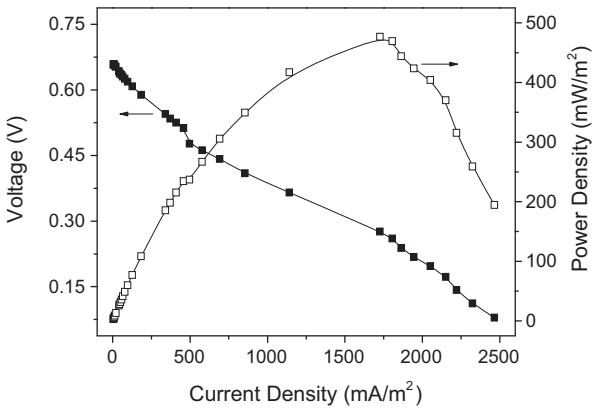

Fig. 2. MFC polarization curve and power density curve.

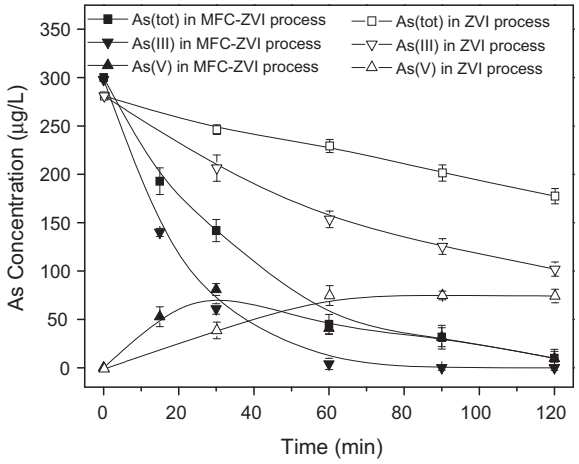

Fig. 3. Arsenic removal in the MFC–ZVI hybrid process and the ZVI process.

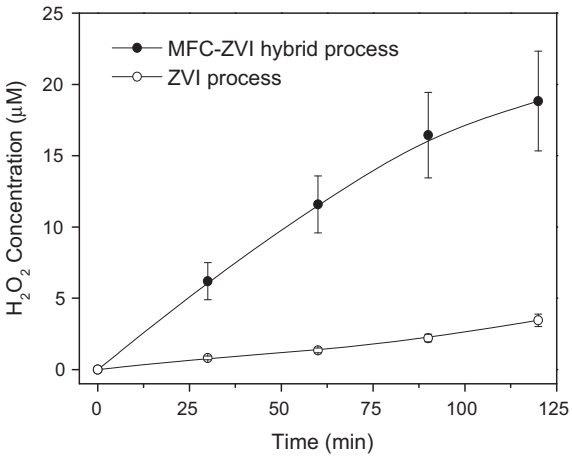

Fig. 4. The concentrations of H_2O_2 generated in the presence of 4 μM BPY in the MFC–ZVI hybrid process and the ZVI process.

residual of 180 μg/L As(tot) and 106 μg/L As(III) in the solution after 2 h, which corresponds to merely 40% removal efficiency of As(tot).

The inflexion points in the As(V) curves can be explained by two competing processes contributing to the As(V) concentrations in the sample. The As(V) is generated via the oxidation of As(III) but simultaneously removed by the ZVI process. Several reactions, such as the generation of oxidants, iron corrosion, and hydrolysis of Fe^{2+}, are involved in the entire processes. At the beginning of the treatment, the As(V) generation rate is higher than its removal rate, which results in the increase of the As(V) concentration in the solution. As the reactions proceed, the As(III) in solution decreases while the amount of HFOs generated increases. As a consequence, the As(V) generation rate gradually decreases and meanwhile its removal speed gradually increases. The As(V) concentration in the solution reaches its maximum when the two rates are equal. After that point, the As(V) removal rate exceeds its generation rate, resulting in the decrease of the As(V) concentration remaining in the solution. For the MFC–ZVI hybrid process, the inflexion point of the As(V) curve appears after around 30 min. Conversely, for the ZVI process, the As(V) concentration increases slowly during the first 60 min before reaching a plateau. The differences in the aqueous As(V) concentration in the two processes indicate that the coupling of ZVI with the MFC accelerates both the oxidant generation and the iron corrosion, which consequently improve the arsenic removal in the hybrid process.

The As(III) removal with a long treatment time and at different pH values in the ZVI process and the MFC–ZVI hybrid process are detailed in Supporting information.

3.3. H_2O_2 generation

H_2O_2, one of the oxidants generated in the ZVI process, was measured after the addition of BPY to prevent the reactions between Fe(II) and oxidants (Fig. 4). The H_2O_2 concentrations in both MFC–ZVI hybrid process and ZVI process increase with time. More H_2O_2 is generated in the MFC–ZVI hybrid process than in the ZVI process over time. The H_2O_2 generation rate in the MFC–ZVI hybrid process is 11.6 μM/h during 0–60 min, which is 9 times higher than that in the ZVI process (1.3 μM/h). After 120 min, the H_2O_2 concentration is 18.8 μM in the MFC–ZVI hybrid process and 3.4 μM in the ZVI process.

The obvious differences in arsenic removal efficiency between the MFC–ZVI hybrid process and the ZVI process, especially the As(V) concentration difference during 0–30 min, strongly depend on the H_2O_2 generation. H_2O_2 can be transformed into stronger oxidizing derivatives in the presence of Fe(II). For example, •OH is generated from H_2O_2 in the acidic condition (pH 3–5) and Fe(IV) is generated via the oxidation of Fe(II) by H_2O_2 in the alkalescent condition (pH 7–9) [44]. The stronger oxidizing derivatives, produced in situ, can oxidize As(III) to As(V) more effectively. Conventionally, preoxidation by adding external oxidants is the requisite step in order to guarantee the effective As(III) removal in the reducible water. The in situ oxidant generation pathway could simplify the operation and reduce the production cost.

3.4. Fe generation

The adsorption and coprecipitation mechanisms involving the HFO generated from the dissolved Fe(II) play important roles in the arsenic removal process. Both As(III) and As(tot) concentrations decrease with the increase of the Fe(tot) in the two processes (Fig. 5). The inset in Fig. 5 shows that the Fe(tot) generation rate in the MFC–ZVI hybrid process is much higher than that in the ZVI process, presumably because the current produced in the MFC process accelerates the iron corrosion. The current efficiency was determined to be 72.7% in this work. Compared with the ZVI process, the removal efficiencies of both As(III) and As(V) are higher in the MFC–ZVI process at the same Fe(tot) concentration.

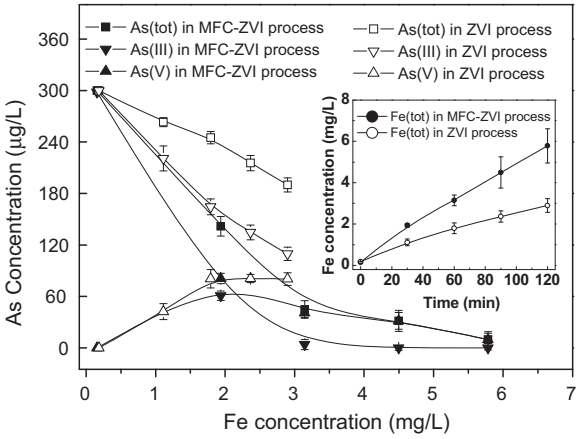

Fig. 5. Effect of Fe(tot) on arsenic removal in the MFC–ZVI hybrid process and the ZVI process. The inset shows the Fe(tot) generation rate in the two processes.

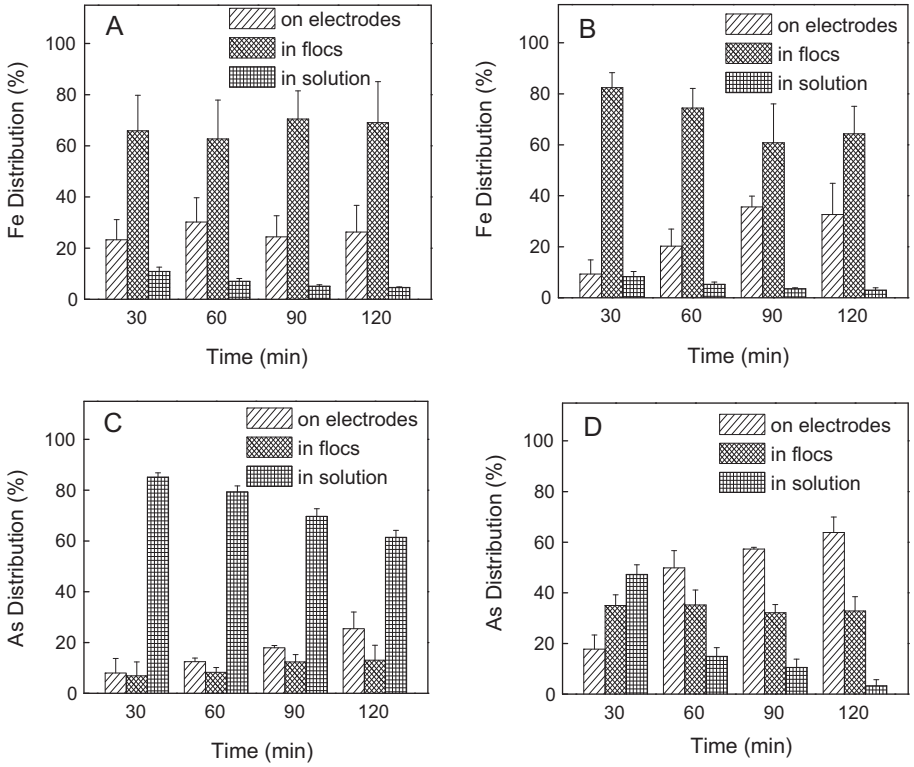

Fig. 6. Fe and As distribution in the processes: Fe in the ZVI process (A), Fe in the MFC–ZVI hybrid process (B), As in the ZVI process (C), and As in the MFC–ZVI hybrid process (D).

3.5. As and Fe distribution

Arsenic or iron is present in three states: in solution, on the electrodes and in the flocs. The Fe generated in both MFC–ZVI and ZVI processes is mainly turned into the flocs in solution (60–80%), while that restricted on the electrodes was around 20% (Fig. 6A and B). Only little Fe is dissolved in solution due to the small disassociation constants of HFOs. According to the As distribution (Fig. 6C and D), both the flocs and the electrodes play important roles in the arsenic removal.

The arsenic removal capability of the flocs in solution can be characterized by the As/Fe molar ratio of the flocs. As shown in Fig. 7, the As/Fe molar ratios decrease with time in both the MFC–ZVI and ZVI processes, which can be explained by the decreasing arsenic concentrations in solution and increasing amounts of HFOs with time. The MFC–ZVI hybrid process has a higher As/Fe molar ratio of the flocs in solution than the ZVI process in most cases, suggesting that the flocs in the MFC–ZVI hybrid process exhibit stronger arsenic removal capability. The value of the As/Fe molar ratio of the flocs in solution depends on the species and concentrations of both the arsenic and the HFOs generated in the system [15,45–47]. The ZVI corrosion products include lepidocrocite, magnetite/maghemite, akaganeite, goethite, etc. [15,45]. As(V) is generally easier to be adsorbed by these corrosion products than As(III). For example, magnetite and hematite can adsorb As(V) effectively but hardly adsorb As(III) [15]. The higher amount of oxidants generated in the MFC–ZVI hybrid process therefore benefit the oxidation of As(III) to As(V). On the other hand, the species of the iron corrosion products in the MFC–ZVI and ZVI processes would be different because the Fe(II) generation rate and the Fe(II)/Fe(III) molar ratio are different in these two processes [15,46,47]. Different species of the iron corrosion products generally exhibit different arsenic adsorption properties.

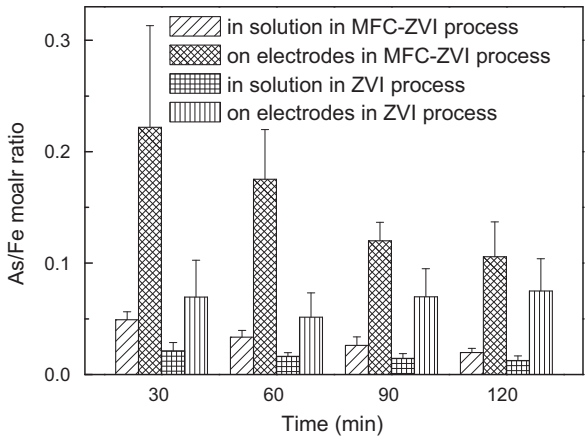

Fig. 7. As/Fe molar ratio of the flocs in solution and on electrodes in the MFC–ZVI hybrid process and the ZVI process.

The higher As/Fe molar ratio of the flocs on the electrodes in the MFC–ZVI hybrid process also suggests higher arsenic removal efficiency by the electrodes (Fig. 7). In the ZVI process alone, the As/Fe molar ratio of the flocs on electrodes stays almost the same as time goes on, which differs from the time dependent trend of the As/Fe molar ratio in the MFC–ZVI hybrid process. The arsenic in the MFC–ZVI hybrid process is presumed to be confined on the electrode surface in two ways, *i.d.* the adsorption by HFOs formed on the electrode surface and the electroadsorption induced by the MFC. Under the experimental pH condition (8.0), $HAsO_4^{2-}$ is the dominant species of As(V) [1]. $HAsO_4^{2-}$ would be driven by the electric field produced by the MFC with an output voltage of about 0.6 V, and be firmly restricted around the iron anode.

Electroadsorption can create a region with higher As(V) concentration in the vicinity of the anode, which would benefit the arsenic adsorption on the iron anode surface through the HFOs. Electroadsorption significantly contributes to the differences in the arsenic removal on the electrodes between the MFC–ZVI hybrid process and the ZVI process.

3.6. Outlook

As(III) is widely distributed in natural water and sediment. As(III) concentrations of more than several hundred mg/kg in sediment and more than several mg/L in surface water have been found [4,5]. Nowadays, SMFCs and BMFCs have been successfully constructed to generate electricity continuously, and some of them have been used to power sensors [23,30,48]. Without other energy input, in situ continuous and effective removal of As(III) from surface water would be realized if the conventional batch MFC in this work is replaced with an SMFC or BMFC. Moreover, arsenic may be immobilized with improved stability by means of the adsorption on HFOs generated in the ZVI corrosion process and the increase of the sediment redox potential resulted from the withdrawal of electrons by the MFC anodes embedded in the sediment.

Compared with some techniques usually used in the wastewater treatment process (e.g., oxidation and coagulation), the MFC–ZVI hybrid process does not possess a high arsenic removal rate. However, since the transformation between As(V) and As(III) and the arsenic transportation between sediment and surface water are slow and long-lasting processes, it is a protracted task to remove As(III) from surface water in situ. Based on this consideration, fast removal is unnecessary and the MFC–ZVI hybrid process would be a good solution to As(III) removal from surface water.

4. Conclusion

An efficient and economical MFC–ZVI hybrid process is successfully developed for the As(III) removal from the aqueous solution. After the water with an arsenite concentration of 300 μg/L was treated for 2 h using the MFC–ZVI hybrid process, the As(tot) concentration remaining in solution was only 9.8 μg/L and the As(III) concentration was below detection limit. The resultant groundwater qualities are compliant with the recommended standards of EPA and WHO.

Compared with the ZVI process, this novel hybrid process is able to generate more oxidants deriving from H_2O_2, which effectively oxidize As(III) to As(V) and further benefit the arsenic removal. The coupling of MFC and ZVI can also accelerate the ZVI corrosion and consequently produce more effective HFOs for the arsenic removal. The electric field produced by the MFC induces an extra electroadsorption force and improves the efficiency of arsenic removal on the electrodes in the MFC–ZVI process. Thanks to these above-mentioned mechanisms, the arsenic removal efficiency in the MFC–ZVI hybrid process is much higher than that in the ZVI process. In addition to arsenic removal, the MFC–ZVI hybrid process can be used to remove other pollutants from surface water, such as phosphate, heavy metals, organic matters, etc.

Acknowledgements

The authors are grateful for the financial support from the National Natural Science Fund (Grant No. 21077001) and the National Five-Year Technology Support Programme (Grant No. 2011BAJ07B04) of China.

Appendix A. Supplementary data

Supplementary data associated with this article can be found, in the online version, at http://dx.doi.org/10.1016/j.jhazmat.2013.07.072.

References

[1] W.R. Cullen, K.J. Reimer, Arsenic speciation in the environment, Chemical Reviews 89 (1989) 713–764.
[2] M. Bissen, F.H. Frimmel, Arsenic-a review. Part I: occurrence, toxicity, speciation, mobility, Acta Hydrochimica et Hydrobiologica 31 (2003) 9–18.
[3] J.Q. Jiang, Removing arsenic from groundwater for the developing world – a review, Water Science and Technology 44 (2001) 89–98.
[4] J.L. Barringer, Z. Szabo, T.P. Wilson, J.L. Bonin, T. Kratzer, K. Cenno, T. Romagna, M. Alebus, B. Hirst, Distribution and seasonal dynamics of arsenic in a shallow lake in northwestern New Jersey, USA, Environmental Geochemistry and Health 33 (2011) 1–22.
[5] J.T. Hollibaugh, S. Carini, H. Gurleyuk, R. Jellison, S.B. Joye, G. LeCleir, C. Meile, L. Vasquez, D. Wallschlager, Arsenic speciation in Mono lake, California: response to seasonal stratification and anoxia, Geochimica et Cosmochimica Acta 69 (2005) 1925–1937.
[6] J.M. Neff, Ecotoxicology of arsenic in the marine environment, Environmental Toxicology and Chemistry 16 (1997) 917–927.
[7] S.J. Santosa, S. Wada, S. Tanaka, Distribution and cycle of arsenic compounds in the ocean, Applied Organometallic Chemistry 8 (1994) 273–283.
[8] J.L. Barringer, A. Mumford, L.Y. Young, P.A. Reilly, J.L. Bonin, R. Rosman, Pathways for arsenic from sediments to groundwater to streams: Biogeochemical processes in the Inner Coastal Plain, New Jersey, USA, Water Research 44 (2010) 5532–5544.
[9] X.H. Guan, H.R. Dong, J. Ma, L. Jiang, Removal of arsenic from water: effects of competing anions on As(III) removal in $KMnO_4$–Fe(II) process, Water Research 43 (2009) 3891–3899.
[10] X.H. Guan, J. Ma, H.R. Dong, L. Jiang, Removal of arsenic from water: effect of calcium ions on As(III) removal in the $KMnO_4$–Fe(II) process, Water Research 43 (2009) 5119–5128.
[11] M. Bissen, F.H. Frimmel, Arsenic – a review. Part II: oxidation of arsenic and its removal in water treatment, Acta Hydrochimica et Hydrobiologica 31 (2003) 97–107.
[12] J.Q. Jiang, Research progress in the use of ferrate(VI) for the environmental remediation, Journal of Hazardous Materials 146 (2007) 617–623.
[13] J.A. Lackovic, N.P. Nikolaidis, G.M. Dobbs, Inorganic arsenic removal by zerovalent iron, Environmental Engineering Science 17 (2000) 29–39.
[14] I.A. Katsoyiannis, T. Ruettimann, S.J. Hug, pH dependence of Fenton reagent generation and As(III) oxidation and removal by corrosion of zero valent iron in aerated water, Environmental Science and Technology 42 (2008) 7424–7430.
[15] B.A. Manning, M.L. Hunt, C. Amrhein, J.A. Yarmoff, Arsenic(III) and Arsenic(V) reactions with zerovalent iron corrosion products, Environmental Science and Technology 36 (2002) 5455–5461.
[16] H.L. Lien, R.T. Wilkin, High-level arsenite removal from groundwater by zerovalent iron, Chemosphere 59 (2005) 377–386.
[17] P. Lai, H.Z. Zhao, C. Wang, J.R. Ni, Advanced treatment of coking wastewater by coagulation and zero-valent iron processes, Journal of Hazardous Materials 147 (2007) 232–239.
[18] B. Lambert, An electrolytic theory of the corrosion of iron, Transactions of the Faraday Society 9 (1913) 108–114.
[19] B.E. Logan, B. Hamelers, R.A. Rozendal, U. Schrorder, J. Keller, S. Freguia, P. Aelterman, W. Verstraete, K. Rabaey, Microbial fuel cells: methodology and technology, Environmental Science and Technology 40 (2006) 5181–5192.
[20] Y. Qiao, S.J. Bao, C.M. Li, X.Q. Cui, Z.S. Lu, J. Guo, Nanostructured polyanifine/titanium dioxide composite anode for microbial fuel cells, Acs Nano 2 (2008) 113–119.
[21] Y. Qiao, C.M. Li, Nanostructured catalysts in fuel cells, Journal of Materials Chemistry 21 (2011) 4027–4036.
[22] J. Liu, Y. Qiao, Z.S. Lu, H. Song, C.M. Li, Enhance electron transfer and performance of microbial fuel cells by perforating the cell membrane, Electrochemistry Communications 15 (2012) 50–53.
[23] C. Donovan, A. Dewan, D. Heo, H. Beyenal, Batteryless, wireless sensor powered by a sediment microbial fuel cell, Environmental Science and Technology 42 (2008) 8591–8596.
[24] C.E. Reimers, P. Girguis, H.A. Stecher, L.M. Tender, N. Ryckelynck, P. Whaling, Microbial fuel cell energy from an ocean cold seep, Geobiology 4 (2006) 123–136.
[25] H. Liu, S.A. Cheng, B.E. Logan, Production of electricity from acetate or butyrate using a single-chamber microbial fuel cell, Environmental Science and Technology 39 (2005) 658–662.
[26] B.E. Logan, Y. Kim, Microbial reverse electrodialysis cells for synergistically enhanced power production, Environmental Science and Technology 45 (2011) 5834–5839.
[27] P. Aelterman, K. Rabaey, H.T. Pham, N. Boon, W. Verstraete, Continuous electricity generation at high voltages and currents using stacked microbial fuel cells, Environmental Science and Technology 40 (2006) 3388–3394.

[28] H.Z. Zhao, Y. Zhang, Y.Y. Chang, Z.S. Li, Conversion of a substrate carbon source to formic acid for CO_2 emission reduction utilizing series-stacked microbial fuel cells, Journal of Power Sources 217 (2012) 59–64.
[29] S.E. Oh, B.E. Logan, Voltage reversal during microbial fuel cell stack operation, Journal of Power Sources 167 (2007) 11–17.
[30] Y.M. Gong, S.E. Radachowsky, M. Wolf, M.E. Nielsen, P.R. Girguis, C.E. Reimers, Benthic microbial fuel cell as direct power source for an acoustic modem and seawater oxygen/temperature sensor system, Environmental Science and Technology 45 (2011) 5047–5053.
[31] H.Z. Zhao, Y. Zhang, B. Zhao, Y.Y. Chang, Z.S. Li, Electrochemical reduction of carbon dioxide in an MFC–MEC system with a layer-by-layer self-assembly carbon nanotube/cobalt phthalocyanine modified electrode, Environmental Science and Technology 46 (2012) 5198–5204.
[32] P. Clauwaert, K. Rabaey, P. Aelterman, L. De Schamphelaire, T.H. Ham, P. Boeckx, N. Boon, W. Verstraete, Biological denitrification in microbial fuel cells, Environmental Science and Technology 41 (2007) 3354–3360.
[33] A.T. Heijne, F. Liu, R.v.d. Weijden, J. Weijma, C.J.N. Buisman, H.V.M. Hamelers, Copper recovery combined with electricity production in a microbial fuel cell, Environmental Science and Technology 44 (2010) 4376–4381.
[34] M. Tandukar, S.J. Huber, T. Onodera, S.G. Pavlostathis, Biological chromium(VI) reduction in the cathode of a microbial fuel cell, Environmental Science and Technology 43 (2009) 8159–8165.
[35] X.X. Cao, X. Huang, P. Liang, K. Xiao, Y.J. Zhou, X.Y. Zhang, B.E. Logan, A new method for water desalination using microbial desalination cells, Environmental Science and Technology 43 (2009) 7148–7152.
[36] M. Mehanna, T. Saito, J.L. Yan, M. Hickner, X.X. Cao, X. Huang, B.E. Logan, Using microbial desalination cells to reduce water salinity prior to reverse osmosis, Energy and Environmental Science 3 (2010) 1114–1120.
[37] D.R. Lovley, E.J.P. Phillips, Novel mode of microbial energy metabolism: organic carbon oxidation coupled to dissimilatory reduction of iron or manganese, Applied and Environment Microbiology 54 (1988) 1472–1480.
[38] M. Rahimnejad, A.A. Ghoreyshi, G. Najafpour, T. Jafary, Power generation from organic substrate in batch and continuous flow microbial fuel cell operations, Applied Energy 88 (2011) 3999–4004.
[39] H. Bader, V. Sturzenegger, J. Hoigne, Photometric-method for the determination of low concentrations of hydrogen-peroxide by the peroxidase catalyzed oxidation of N,N-diethyl-p-phenylenediamine (DPD), Water Research 22 (1988) 1109–1115.
[40] J. Zhu, H.Z. Zhao, J.R. Ni, Fluoride distribution in electrocoagulation defluoridation process, Separation and Purification Technology 56 (2007) 184–191.
[41] H.Z. Zhao, B. Zhao, W. Yang, T.H. Li, Effects of Ca^{2+} and Mg^{2+} on defluoridation in the electrocoagulation process, Environmental Science and Technology 44 (2010) 9112–9116.
[42] Q. Wen, Z.M. Liu, Y. Chen, K.F. Li, N.Z. Zhu, Electrochemical performance of microbial fuel cell with air-cathode, Acta Physico-Chimica Sinica 24 (2008) 1063–1067.
[43] H. Liu, B.E. Logan, Electricity generation using an air-cathode single chamber microbial fuel cell in the presence and absence of a proton exchange membrane, Environmental Science and Technology 38 (2004) 4040–4046.
[44] S.J. Hug, O. Leupin, Iron-catalyzed oxidation of arsenic(III) by oxygen and by hydrogen peroxide: pH-dependent formation of oxidants in the Fenton reaction, Environmental Science and Technology 37 (2003) 2734–2742.
[45] B. Gu, T.J. Phelps, L. Liang, M.J. Dickey, Y. Roh, B.L. Kinsall, A.V. Palumbo, G.K. Jacobs, Biogeochemical dynamics in zero-valent iron columns: implications for permeable reactive barriers, Environmental Science and Technology 33 (1999) 2170–2177.
[46] S. Alibeigi, M.R. Vaezi, Phase transformation of iron oxide nanoparticles by varying the molar ratio of Fe^{2+}:Fe^{3+}, Chemical Engineering and Technology 31 (2008) 1591–1596.
[47] H. Liu, P. Li, M.Y. Zhu, Y. Wei, Y.H. Sun, Fe(II)-induced transformation from ferrihydrite to lepidocrocite and goethite, Journal of Solid State Chemistry 180 (2007) 2121–2128.
[48] B.H. Kim, I.S. Chang, G.C. Gil, H.S. Park, H.J. Kim, Novel BOD (biological oxygen demand) sensor using mediator-less microbial fuel cell, Biotechnology Letters 25 (2003) 541–545.